$|V_{\rm cb}|$ and $|V_{\rm ub}|$ measurements at LEP

Marta Calvi

Dipartimento di Fisica Universitá di Milano Bicocca and INFN Sezione di Milano, Italy
Email: Marta.Calvi@mi.infn.it

ABSTRACT: New measurements have been performed by the four LEP Collaborations with data collected at LEP at the Z^0. The $|V_{\rm cb}|$ element has been determined both from the inclusive method, which uses the semileptonic decay width of b decays, and the exclusive method, by studying the exclusive $\overline{\rm B}^0 \to {\rm D}^{*+}\ell^-\overline{\nu}_\ell$ decay process. The $|V_{\rm ub}|$ element has been determined from inclusive charmless semileptonic b-hadron decays, by studing the invariant mass spectrum of the hadronic system.

1. Introduction

Within the framework of the Standard Model of electroweak interactions, the mixing of quarks in the charged weak interactions is described by the Cabibbo-Kobayashi-Maskawa matrix. The values of the matrix elements are free parameters, constrained only by the requirement that the matrix be unitary. The observed hierarchy in the elements suggested to Wolfenstein the following parametrization:

$$V_{CKM} = \begin{pmatrix} V_{ud} & V_{us} & V_{ub} \\ V_{cd} & V_{cs} & V_{cb} \\ V_{td} & V_{ts} & V_{tb} \end{pmatrix} =$$

$$\begin{pmatrix} 1-\frac{1}{2}\lambda^2 & \lambda & A\lambda^3(\rho-i\eta) \\ -\lambda & 1-\frac{1}{2}\lambda^2 & A\lambda^2 \\ A\lambda^3(1-\rho-i\eta) & -A\lambda^2 & 1 \end{pmatrix} + O(\lambda^4)$$

The four parameters: $\lambda = \sin(\theta_{Cabibbo})$, A, ρ and η have to be measured by experiments. $\eta \neq 0$ is required in order to generate CP violation. The condition of unitarity: $V^\dagger V = 1$ implies relations between the four parameters which can be visualized by triangles in the (ρ , η) plane. A constraint relevant for transitions involving the b quark is derived from the first and the third column of the matrix:

$$V_{ud}V_{ub}^* + V_{cd}V_{cb}^* + V_{td}V_{tb}^* = 0$$

It is related to the triangle drawn in figure 1 where the length of the side CB has been rescaled

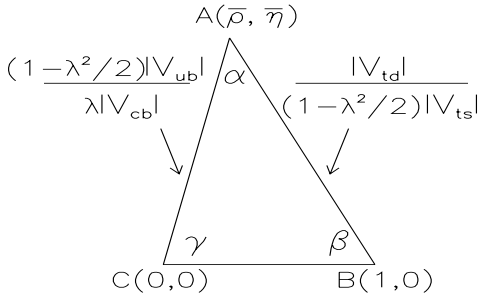

Figure 1: Unitarity triangle in the complex plane.

for $A\lambda^3 = \lambda|V_{cb}|$, and the corrections: $\bar{\rho} = \rho(1-\lambda^2/2)$, $\bar{\eta} = \eta(1-\lambda^2/2)$ have been introduced.

The study of flavour physics, tests of the Standard Model and its possible extensions and understanding the source of CP violation require the knowledge of all sides and angles of the Unitarity Triangle and therefore a precise determination of the matrix elements $|V_{cb}|$ and $|V_{ub}|$.

Theoretical inputs are needed in order to evaluate $|V_{cb}|$ and $|V_{ub}|$ from measured observables. The values and the uncertainties adopted here are those defined at the "Informal Workshop on the Derivation of $|V_{cb}|$ and $|V_{ub}|$: Experimental Status and Theory Uncertainties" held at CERN beginning of June 1999. The conclusions of the Workshop and the related references can be found in [1].

2. $|V_{\rm cb}|$ determination

Two experimental methods are available in order to determine of $|V_{\rm cb}|$ with relatively small theoretical uncertainties: the **inclusive** method, which uses the semileptonic decay width of b decays, and the **exclusive** method, where $|V_{\rm cb}|$ is extracted by studying the exclusive $\overline{\rm B}^0 \to {\rm D}^{*+}\ell^-\overline{\nu}_\ell$ decay process.

2.1 $|V_{\rm cb}|$ determination from inclusive $b \to X\ell\nu$ decays

In the inclusive determination, the partial width for semileptonic B mesons decays to charmed mesons is related to $|V_{\rm cb}|$ by [1]:

$$\Gamma(B \to X_c\ell\nu) = \frac{G_F}{192\pi^3} m_b^5 |{\rm V_{cb}}|^2 f(\frac{m_c}{m_b}, \frac{m_\ell}{m_b})\gamma_c$$

where f is a known phase space factor, depending on the b and the c quark masses, and γ_c represents perturbative and non perturbative corrections to the muon decay formalism.

Experimentally, the semileptonic width is determined from the semileptonic branching ratio and the lifetime:

$$\Gamma(B \to X_c l\nu) = \frac{BR(B \to X_c\ell\nu)}{\tau_{\rm B}}.$$

In Z^0 decays B^0, B^-, B_s and b-baryons are produced, so the inclusive semileptonic branching ratio measured at LEP is an average over the different produced hadrons. Assuming that all b-hadrons have equal semileptonic width, the following relation holds:

$$\begin{aligned} BR(b \to X_c\ell\nu)_{LEP} &= \Gamma(B \to X_c\ell\nu) \times \\ &(f_{B^0}\tau_{B^0} + f_{B^-}\tau_{B^-} + f_{B_s}\tau_{B_s} + f_{\Lambda_b}\tau_{\Lambda_b}) \\ &= \Gamma(B \to X_c\ell\nu) \times \tau_b \end{aligned} \quad (2.1)$$

where $f_{B^0}, f_{B^-}, f_{B_s}$ and f_{Λ_b} are the production fractions of B^0, B^-, B_s mesons and b-baryons respectively, and $\tau_b = f_{B^0}\tau_{B^0} + f_{B^-}\tau_{B^-} + f_{B_s}\tau_{B_s} + f_{\Lambda_b}\tau_{\Lambda_b}$ is the average b-hadron lifetime. Therefore the semileptonic width can be obtained at LEP using the inclusive semileptonic branching ratio and the average b-hadron lifetime. The hypothesis of equal semileptonic width may be incorrect for b-baryons. Taking into account the present precision of LEP measurements of b-baryon semileptonic branching ratios and lifetimes, the maximal possible correction to equation 2.1 is about 2%.

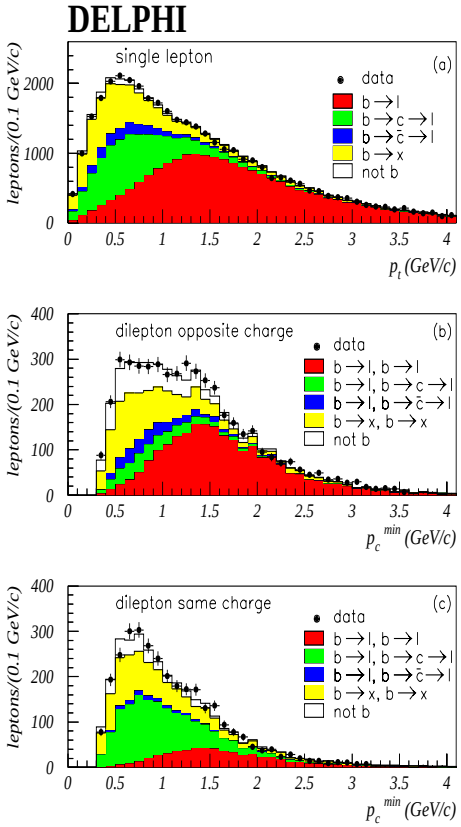

Figure 2: DELPHI preliminary results. Comparison of data and simulation spectra. The simulation spectra have been reweighted according to the result of the fit. (a) Transverse momentum distribution for single electrons and muons. (b) Combined momentum distribution for the two leptons in di-lepton events, identified in opposite jets and having an opposite charge. (c) Combined momentum distribution for the two leptons in di-lepton events, identified in opposite jets and having the same charge. In (b) and (c) the p_c^{min} refers to the minimum combined momentum of the two leptons.

The DELPHI Collaboration has presented this summer preliminary results [3] on the inclusive semileptonic branching ratios of b-hadrons. Three inclusive branching ratios are measured: the direct BR($b \to \ell$) and the two cascade

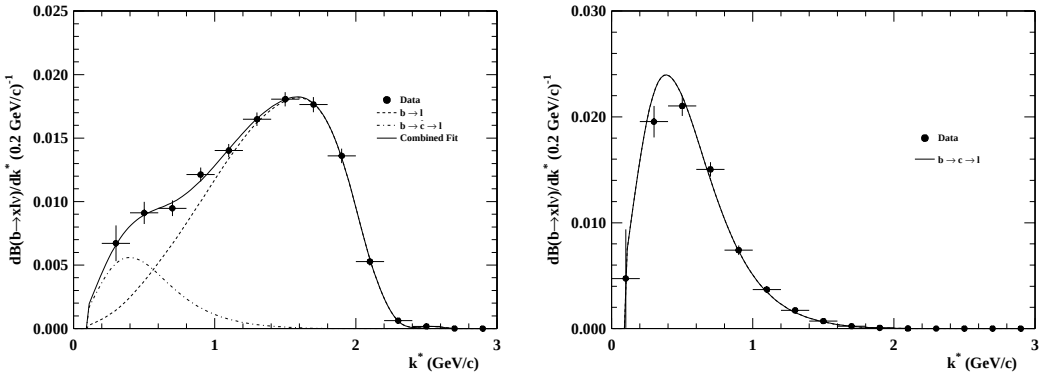

Figure 3: DELPHI preliminary results. Lepton momentum spectra in the b-hadron rest frame. The left (right) plot shows the result of the fit with the ACCMM model to the like-sign (opposite-sign) sample.

BR($b \to c \to \ell$) and BR($b \to \bar{c} \to \ell$).

Four different analyses are performed, only two are described here. In the first, single lepton spectra are studied in a sample of pure $b\bar{b}$ events, selected by means of a b-flavour lifetime tagging algorithm, applied to the hemisphere opposite to the lepton. A $b\bar{b}$ purity of 95% with an efficiency of 39% is achieved. A sample of di-leptons in opposite jets is also used, where an enriched $b\bar{b}$ purity is obtained by requiring a minimum transverse momentum of one of the two leptons. The sensitivity to the different sources of leptons is given by the kinematic properties of leptons from different sources and by the charge correlation between di-leptons in opposite jets from b and $\bar{b}$ respectively. The branching ratios are extracted from a maximum likelihood fit of the Monte Carlo expectations to the data. The lepton spectra are shown in figure 2.

In the second DELPHI analysis the inclusive reconstruction of the charge and the momentum of the b-hadron system is performed. In a sample of events enriched in $b\bar{b}$ purity by means of a lifetime b-flavour tag, B decay vertices are reconstructed. For each charged particle a probability that the particle originated from the b-hadron decay vertex, rather than from fragmentation, is calculated using an artificial neural network. Using these probabilities, a vertex charge is calculated. The correlation between the lepton charge and the b-hadron charge is used to separate direct from cascade leptons. The b-hadron momentum is also reconstructed with a resolution of 7%. Lepton momenta are fitted after boosting into the b rest frame. Results are shown in figure 3.

The DELPHI results for the combination of all analyses are:

$$\begin{aligned} BR(b \to \ell) &= (10.65 \pm \\ 0.07(stat) \pm 0.25(\ syst\ )^{+0.42}_{-0.28}(model)) &\times 10^{-2} \\ BR(b \to c \to \ell) &= (7.88 \pm \\ 0.13(stat) \pm 0.27(\ syst\ )^{+0.32}_{-0.38}(model)) &\times 10^{-2} \\ BR(b \to \bar{c} \to \ell) &= (1.71 \pm \\ 0.13(stat) \pm 0.36(\ syst\ )^{+0.19}_{-0.25}(model)) &\times 10^{-2} \end{aligned}$$

The main contributions to the systematic errors are the uncertainties in the lepton efficiencies and misidentification probabilities, uncertainties related to the b-flavour tagging procedures and uncertainties in the reconstruction and fitting procedures. The uncertainties due to the semileptonic decay model are given separately.

The inclusive measurement of the OPAL Collaboration [4] also uses lifetime techniques to suppress the contribution from non-$b\bar{b}$ events. A sample of hemispheres containing a b-hadron is selected with a purity of 92% and an efficiency of 30%. A search for lepton candidates is made in the hemisphere opposite to a b-tagged hemisphere. Jet shape and momentum variables are used in two artificial neural networks NN_{bl} and NN_{bcl} trained respectively to distinguish direct decays and cascade decays from all other sources of leptons. The distributions of the neural networks outputs are compared for the data and the Monte Carlo and a binned maximum like-

lihood fit is performed to determine the fraction of events coming from direct and cascade decays. The network outputs are shown in figure 4.

The results are:

$$\begin{aligned} BR(b \to \ell) &= (10.83 \pm \\ 0.10(stat) \pm 0.20(\ syst\ )^{+0.20}_{-0.13}(model)) &\times 10^{-2} \\ BR(b \to c \to \ell) &= (8.40 \pm \\ 0.16(stat) \pm 0.21(\ syst\ )^{+0.33}_{-0.29}(model)) &\times 10^{-2} \end{aligned}$$

The new measurement of the L3 Collaboration [5] is a combined measurement of $R_b = \Gamma(Z \to b\bar{b})/\Gamma(Z \to hadrons)$ and the semileptonic branching ratio, using a double tag technique. An event is split into two hemispheres defined by the plane normal to the thrust axis and for each hemispheres two criteria are applied in order to enhance the b purity: one is based on lifetime and the other on high p_t leptons. The number of tagged hemispheres, N_t, is related to the total number of hadronic events, N_{had}, by the following equation:

$$\frac{N_t}{2N_{had}} = R_b\epsilon_b + R_c\epsilon_c + (1 - R_c - R_b)\epsilon_{uds}$$

where ϵ_b, ϵ_c and ϵ_{uds} are the tagging efficiencies for b, c and light quark hemispheres. The number of events with both hemispheres tagged, N_{tt}, is given by:

$$\frac{N_{tt}}{N_{had}} = c_b R_b \epsilon_b^2 + c_c R_c \epsilon_c^2 + c_{uds}(1 - R_c - R_b)\epsilon_{uds}^2$$

where the additional factors c_b, c_c and c_{uds} quantify residual correlations between the two hemispheres. If a different b-flavour tagging algorithm is applied, three additional equations can be derived:

$$\begin{aligned} \frac{N_{t'}}{2N_{had}} &= R_b\epsilon'_b + R_c\epsilon'_c + (1 - R_c - R_b)\epsilon'_{uds} \\ \frac{N_{t't'}}{N_{had}} &= c'_b R_b \epsilon'^2_b + c'_c R_c \epsilon'^2_c + \\ &\quad c'_{uds}(1 - R_c - R_b)\epsilon'^2_{uds} \\ \frac{N_{tt'}}{N_{had}} &= c''_b R_b \epsilon_b \epsilon'_b + c''_c R_c \epsilon_c \epsilon'_c + \\ &\quad c''_{uds}(1 - R_c - R_b)\epsilon_{uds}\epsilon'_{uds} \end{aligned}$$

The measurements are used to determine the values of R_b, ϵ_b and ϵ'_b, while $c_b, \epsilon_c, \epsilon_{uds}, c'_b, \epsilon'_c, \epsilon'_{uds}, c''_b$ are constrained to the values obtained from the Monte Carlo simulation. The efficiency ϵ'_b quantifies the fraction of high p, p_t leptons in a b-jets. Therefore it is sensitive to the value of semileptonic branching ratio of b-hadrons. This is obtained from the comparison of the measured efficiency and the Monte Carlo reference one. The final result is:

$$\begin{aligned} BR(b \to \ell) &= (10.16 \pm \\ &0.13(stat) \pm 0.27(syst)) \times 10^{-2} \end{aligned} \quad (2.2)$$

The average LEP value for the BR($b \to \ell$) is obtained from a global fit which combines all the semileptonic branching ratios measurements at LEP and the other correlated heavy flavour measurements performed at LEP; namely the measurements of the average $B^0 - \bar{B}^0$ mixing parameter and R_b [2]. In addition to the three presented measurements of branching ratios, also the preliminary ALEPH measurement [6] and the previous L3 measurement [7] are included. The result for the average BR($b \to \ell$) at LEP is:

$$\begin{aligned} BR(b \to \ell) &= (10.58 \pm \\ &0.07(stat) \pm 0.17(syst)) \times 10^{-2} \end{aligned} \quad (2.3)$$

The χ^2 of the fit is 10.8/(17-5).

The largest single contribution to the systematic error is the uncertainty related to the semileptonic decay model, which amounts to 0.08×10^{-2}. A model is needed to describe the lepton spectra below the momentum cut. Thanks to the boost of b quarks from Z^0 decays, the lepton momentum cut, performed in the laboratory frame, has a reduced importance with respect to similar analyses performed on b-hadrons at rest. However the momentum resolution is diluted. Both OPAL and L3 have performed fits with the aim of constraining different semileptonic decay models. The sensitivity doesn't seem to be sufficient to rule out a specific model, but clear indications are seen, as the fact that a contribution of more than 20% for leptons originating from D**decays is needed. Additional studies are going on in the ALEPH and DELPHI Collaborations.

The $|V_{\rm cb}|$ value is determinated from the inclusive branching ratio using the HQET results [8, 1]:

$$|\mathrm{V_{cb}}| = 0.0411 \sqrt{\frac{BR(b \to X_c \ell \nu)}{0.105} \frac{1.55}{\tau_b}} \times$$

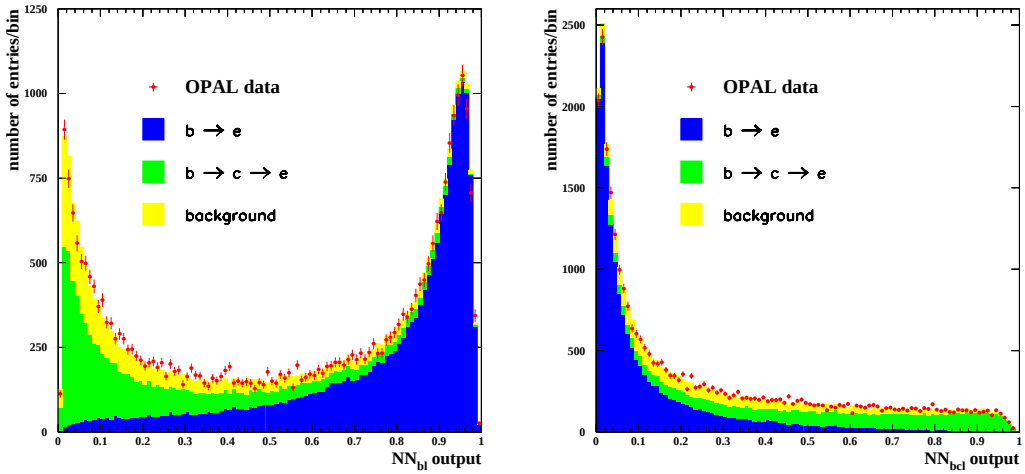

Figure 4: Distribution of the output variable for the neural networks NN_{bl} and NN_{bcl} for electrons. The separate contributions of $b \to \ell$, $b \to c \to \ell$ and background are shown.

$$\left(1 - 0.024\left(\frac{\mu_\pi^2 - 0.5}{0.1}\right)\right) \times$$
$$(1 \pm 0.030(pert) \pm 0.020(m_b) \pm 0.024(\frac{1}{m_Q^3}))$$

The $BR(b \to X_u \ell\nu)$ contribution is subtracted from $BR(b \to X\ell\nu)$ using the LEP average value of section 3 and the world average value of the b-hadron lifetime [23]:

$$\tau_b = 1.564 \pm 0.014\ ps \qquad (2.4)$$

is used. The result is:

$$|\mathrm{V_{cb}}| = (40.75 \pm 0.41(exp) \pm 2.04(theo)) \times 10^{-3}$$

where the first error is experimental and the second from theory. The contributions to the experimental error of the error on the semileptonic branching ratio and the error on the lifetime are $\pm 0.37 \times 10^{-3}$ and $\pm 0.18 \times 10^{-3}$, respectively.

2.2 $|V_{\mathrm{cb}}|$ determination from exclusive decays $\overline{\mathrm{B}}^0 \to \mathrm{D}^{*+}\ell^-\overline{\nu}_\ell$

In the exclusive determination, the value of $|V_{\mathrm{cb}}|$ is extracted by studying the decay rate for the process $\overline{\mathrm{B}}^0 \to \mathrm{D}^{*+}\ell^-\overline{\nu}_\ell$ as a function of the recoil kinematics of the D^{*+} meson. The decay rate is parameterized as a function of the variable w, defined as the product of the four velocities of the D^{*+} and the $\overline{\mathrm{B}}^0$ mesons. This is related to the square of the four momentum transfer from the $\overline{\mathrm{B}}^0$ to the $\ell^-\overline{\nu}_\ell$ system, q^2, by:

$$w = \frac{m_{\mathrm{D}^{*+}}^2 + m_{\mathrm{B}^0}^2 - q^2}{2 m_{\mathrm{B}^0} m_{\mathrm{D}^{*+}}} \qquad (2.5)$$

and ranges from 1.0, when the D^{*+} is produced at rest in the $\overline{\mathrm{B}}^0$ rest frame, to about 1.5. Using HQET, the differential partial width for this decay is given by:

$$\frac{\mathrm{d}\Gamma}{\mathrm{d}w} = \mathcal{K}(w)\mathcal{F}^2(w)|V_{\mathrm{cb}}|^2$$

where $\mathcal{K}(w)$ is a known phase space term and $\mathcal{F}(w)$ is the hadronic form factor for the decay. Although the shape of this form factor is not known, its magnitude at zero recoil, $w = 1$, can be estimated using HQET. In the heavy quark limit ($m_{\mathrm{b}} \to \infty$), $\mathcal{F}(w)$ coincides with the Isgur-Wise function $\xi(w)$ [9, 10] which is normalised to unity at the point of zero recoil. Corrections to $\mathcal{F}(1)$ have been calculated to take into account the effects of finite quark masses and QCD corrections [11]. Calculations of this correction yield [1]:

$$\mathcal{F}(1) = \left(0.88 - 0.024\left(\frac{\mu_\pi^2 - 0.5}{0.1}\right)\right) \times$$
$$(1 \pm 0.035(excit) \pm 0.010(pert) \pm 0.025(\frac{1}{m^3}))$$
$$= 0.88 \pm 0.05$$

Since the phase space factor $\mathcal{K}(w)$ tends to zero as $w \to 1$, the decay rate vanishes at $w = 1$ and a fit of the differential decay rate distribution is performed over the whole kinematic range. The accuracy of the extrapolation relies on achieving a reasonably constant reconstruction efficiency in the region about $w = 1$. The unknown function $\mathcal{F}(w)$ is approximated with an expansion around $w = 1$. First measurements of $|V_{\rm cb}|$ were performed assuming a linear expansion, i.e. neglecting the second order terms. A positive curvature is however predicted from basic considerations, and a relation between the slope and the curvature [12] was used as a constraint in later measurements. An improved parametrization was recently proposed [13]. A novel function $\mathcal{A}_1(w)$ was introduced, and the following approximation obtained:

$$\mathcal{A}_1(w) = \mathcal{A}_1(1) \times \{1 - 8\rho^2_{\mathcal{A}} z + (53\rho^2_{\mathcal{A}} - 15)z^2 - (231\rho^2_{\mathcal{A}} - 91)z^3\} \qquad (2.6)$$

where $\rho_{\mathcal{A}}$ is the slope parameter at zero recoil and $z = (\sqrt{w+1} - \sqrt{2})/(\sqrt{w+1} + \sqrt{2})$. In the limit $w \to 1$, $\mathcal{A}_1(w) = \mathcal{F}(w)$, so that $\mathcal{A}_1(1) \simeq \mathcal{F}(1)$.

The most recent result on exclusive decays is from the DELPHI Collaboration [20]. An inclusive reconstruction of the $\mathrm{D}^{*+}\ell^-$ system is performed by tagging the slow π emitted in the $\mathrm{D}^{*+} \to D^0\pi^+$ decay. The pion charge is required to be opposite to that of the lepton. The mass difference $\Delta m = M_{D\pi} - M_D$ is shown in figure 5; all events with $\Delta m < 0.165$ GeV/c^2 were used as D^{*+} candidates. The shape of the combinatorial background is well described by events with the π and the lepton having the same charge.

The w variable is reconstructed as in equation 2.5, where q^2 is obtained from $q^2 = (p_{\bar{B}^0} - p_{D^{*+}})$. To improve the resolution on w the squared recoil mass was also determinated, on the basis of the event kinematics. It represents the square of the mass of the neutrino and its value was constrained to zero. With this procedure only 5% of the events were reconstructed outside the allowed kinematic range $1 < w < 1.504$. A minimum χ^2 fit was performed, comparing the number of observed and expected events. The parametrization of equation 2.6 was used to describe the signal, obtaining:

$$\mathcal{A}_1(1)|V_{\rm cb}| = (37.95 \pm 1.34_{stat} \pm 1.59_{syst}) \times 10^{-3}$$
$$\rho^2_{\mathcal{A}} = 1.39 \pm 0.12_{stat} \pm 0.18_{syst}$$

The fit to the w distribution is shown in figure 6.

In order to extract the differential decay width and the function $\mathcal{A}_1$, an unfolding procedure was applied to the data, to cope with the non-negligible smearing due to the experimental resolution. The result for $d\Gamma/dw$ is shown in figure 7.

In this and other D^{*+} analyses, the dominant source of physics background is the contamination from intermediate charmed excited states, collectively called D^{**}, which then decay to a D^{*+}; as an example, $B^- \to D^{**0}\ell^-\bar{\nu}$ with $D^{**0} \to D^{*+}\pi^-$. Evidence for the production of resonant states D_1 and D_2^* have been reported by the ALEPH [17] and CLEO [16] collaborations.

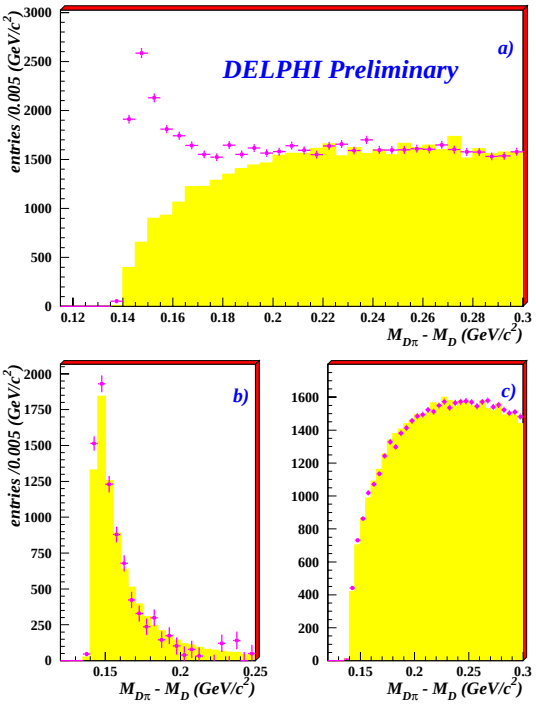

Figure 5: DELPHI preliminary results. Mass difference $\Delta m = M_{D\pi} - M_D$. (a) opposite charge, data (crosses), same charge (shaded area). (b) opposite charge, data after subtraction of the combinatorial background (crosses), resonant contribution from simulation (shaded area) (c) simulation: combinatorial background from opposite charge (crosses) compared to the equal charge combination, normalized in the side band.

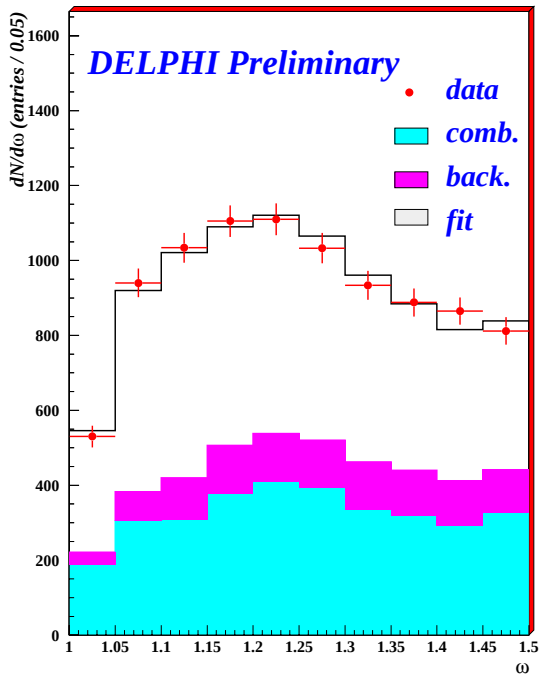

Figure 6: DELPHI preliminary results. Fit to the w distribution. Data (dots), combinatorial background (light shaded area), other backgrounds including D^{**} (dark shaded area) and signal $\overline{B}^0 \to D^{*+}\ell^-\overline{\nu}_\ell$ (white area).

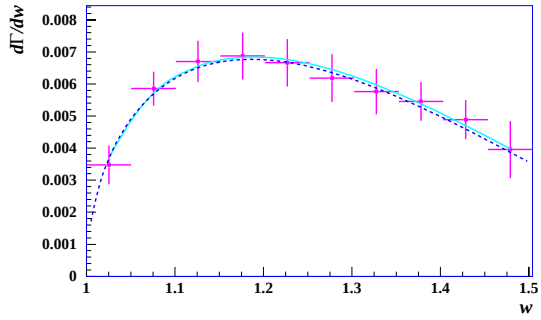

Figure 7: DELPHI preliminary results. Unfolded distribution of the differential decay width. The continuous line shows the result of a fit to the histogram, neglecting bin to bin correlations. The dotted line shows the result obtained when including the statistical correlations among the bins.

Non-resonant states have not been identified at present. Inclusive measurements of the decays $B \to D^*\ell\bar{\nu}X$ have however been performed by the ARGUS [18], ALEPH [17] and DELPHI [19] collaborations using different techniques.

A precise description of the D^{**} form factors is also required. Different models give non-negligible differences in the results. Published results are based on the old Isgur-Wise model, which overestimates the rate of background near the spectrum end point. Indeed, HQET predicts that in the infinite charm mass limit, the rate near $w = 1$ is suppressed by a further factor $(w^2 - 1)$ when compared with the signal [15]. However, models in this extreme case fail to predict the fraction of resonant D^{**} states. A more precise treatment which accounts for $\mathcal{O}(1/m_c)$ corrections is proposed in [14]. Several possible approximations of the form factors are provided. To be conservative, at the present stage of the analysis, the LEP systematic error due to the modelling of the D^{**} background was computed as half the difference between the two extreme results obtained varying all the input parameters in [14] over their full range. Future improvements in this field are envisaged, both from new experimental measurements of charmed excited states, and from theory.

In the LEP average value of $|V_{cb}|$, the published ALEPH [21] and OPAL[22] measurements are included. Since the three LEP measurements have been performed using different methods and inputs, they must be brought onto the same footing before being averaged. They have been updated by the LEP working group [1] to use the Caprini-Lellouch-Neubert [13] extrapolating method, the Ligeti [14] $\overline{B}^0 \to D^{**}\ell^-\overline{\nu}_\ell$ model and the same physics input parameters (such as b-hadron production rates, charm branching ratios, etc.). Table 1 lists the corrected results for the three experiments.

After combining the above results, the LEP average is:

$$\mathcal{F}(1)|V_{cb}| = (33.8 \pm 0.9(stat) \pm 1.9(syst)) \times 10^{-3}$$
$$\rho^2_{\mathcal{A}} = 1.00 \pm 0.09 \pm 0.14$$

The dominant systematic errors on $\mathcal{F}(1)|V_{cb}|$ are listed in table 2.

The confidence level of the fit is 15%. The error ellipse of the corrected measurement and of the LEP average is shown in figure 8.

Using the theoretical estimate $\mathcal{F}(1)$=0.88 $\pm$ 0.05, the $|V_{cb}|$ average is:

$$|V_{cb}| = (38.4 \pm 1.1(stat) \pm 2.2(syst) \pm 2.2(theo)) \times 10^{-3}.$$

experiment	$\mathcal{F}(1)\|V_{cb}\|$ ($\times 10^{-3}$)	$\rho^2_{\mathcal{A}}$
ALEPH	32.2± 2.1± 1.6	0.6± 0.3± 0.1
DELPHI	36.3± 1.4± 2.5	1.4± 0.1± 0.3
OPAL	34.2± 1.9± 2.7	1.1± 0.2± 0.2

Table 1: Experimental results corrected to the common inputs.

Source	$\mathcal{F}(1)\|V_{cb}\|$ (%)	$\rho^2_{\mathcal{A}}$
$Br(D \to Kn\pi)$	1.0	0.01
$Br(D^{*+} \to D^0\pi^+)$	1.0	-
$\Gamma_{b\bar{b}}/\Gamma_{had}$	0.18	-
$Br(b \to B^0)$	1.6	-
$B^- \to D^* X \ell\bar{\nu}$	4.5	0.16
$\bar{B} \to D^* X_c$	0.18	-
$\bar{B} \to D^* \tau\bar{\nu}$	0.25	-
Detector	2.1	0.10
Fragmentation	0.9	-
B^0 lifetime	1.6	-
Total syst.	5.7	0.19
Statistical	2.7	0.09

Table 2: The dominant systematic errors on $\mathcal{F}(1)|V_{cb}|$.

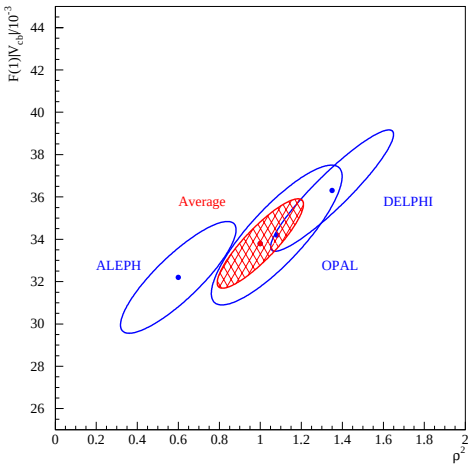

Figure 8: Error ellipses (1 sigma) of the corrected measurements and LEP average $|V_{cb}|$ using the exclusive method.

2.3 Inclusive and exclusive $|V_{cb}|$ average

The inclusive and exclusive measurements are highly independent and can be averaged obtaining a $|V_{cb}|$ value with a total error smaller than 5%. Indeed $|V_{cb}|$ is now the second best measured parameter of the CKM matrix, after λ. The average, as shown in figure 9, is:

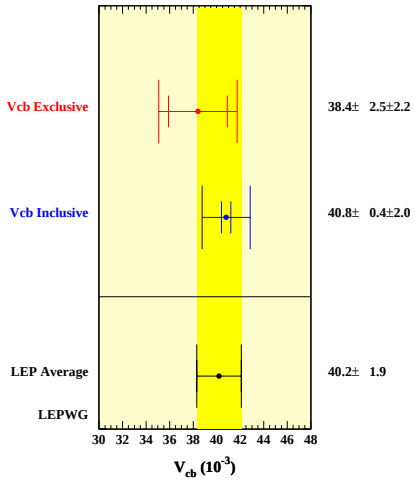

Figure 9: $|V_{cb}|$ LEP average from inclusive and exclusive methods

$$|V_{cb}| = (40.2 \pm 1.9) \times 10^{-3} \qquad (2.7)$$

where within the total error of 1.9, 1.5 comes from uncorrelated sources and 1.2 from correlated sources. The most important source of correlations between the inclusive and exclusive methods comes from theoretical uncertainties in the evaluation of μ_π [1]. For the experimental systematic errors, theoretical uncertainties in the modelling of $b \to \ell$ decays and the exact amount of $b \to D^{**}$decays are taken as fully correlated.

3. $|V_{ub}|$ determination

The isolation of b quark decays to charmless states is not an easy task, since the charmed decays, which we have just considered in the previous section, have a rate larger by about two orders of magnitude. Semileptonic transitions $b \to X_u \ell\nu$ are usually studied, where X_u may represent any

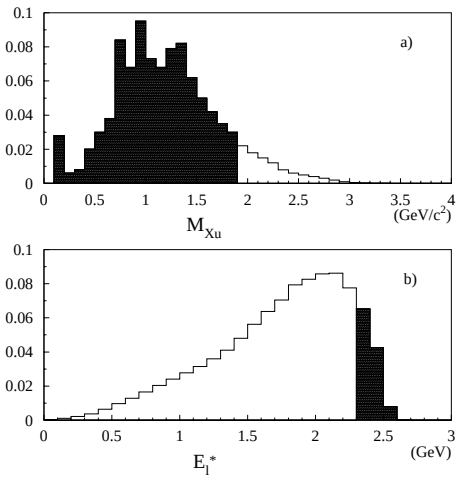

Figure 10: (a) Hadronic invariant mass distribution in $b \to X_u \ell\nu$ decays and (b) lepton momentum distribution calculated in the b-hadron rest frame. In the two plots the shaded area indicates the region inaccessible to $b \to c$ transitions.

charmless state, like π, η, ω, $\pi\pi$, $\pi\pi\pi$, etc. Exclusive searches, such as $B \to \pi\ell\nu$ or $B \to \rho\ell\nu$ have an experimentally well defined strategy, based on mass peak reconstruction. However large theoretical uncertainties affect the evaluation of the transition amplitudes, leading to a model dependent measurement of the matrix element $|V_{\rm ub}|$. Inclusive measurements are thus pursued. These are experimentally more difficult, because the reconstruction of all decay particles in the event is needed, but theoretical calculations are available with an uncertainty of about only 5%. At the $\Upsilon(4S)$ a clear signal of charmless semileptonic decays has been found in an excess of events in the end-point region of the lepton momentum distribution, above charm threshold (2.3 GeV/c$< p <$ 2.6 GeV/c). However, in order to extract the value of $|V_{\rm ub}/V_{\rm cb}|$, an extrapolation is needed from this small phase space region to the low momentum region, leading again to a model dependent measurement. Kinematics at LEP are different: the boost of the b-hadrons and the good separation of the two initial state quarks imply back to back decay products that hardly mix. As a consequence, the hadronic system in $b \to X_u \ell\nu$ candidates can be analyzed, and an extended phase space region can be studied, reducing the model dependence of the result. As shown in figure 10 from reference [25], 90% of $b \to X_u \ell\nu$ decays are expected to have an invariant mass $M_{X_u} < 1.87$ GeV/c^2, below charm threshold, while only 10% of these decays have a lepton with energy E_ℓ^* above the kinematic boundary for $b \to c$ transitions.

The other sources of background to the $b \to X_u \ell\nu$ signal are: hadronic b decays to charmed hadrons which then undergo semileptonic decay, hadronic Z^0 decays to charm or light quarks and possible lepton misidentification in the full sample of hadronic Z^0 decays. All these sources of background are largely depleted by the same selection criteria devised to enhance the ratio between $b \to X_u \ell\nu$ and $b \to X_c \ell\nu$ events.

In the ALEPH [25] analysis, events with a candidate lepton are selected and a lifetime b tag is applied to the hemisphere opposite to the lepton one. Particles originating from the hadronic system X_u are selected using two artificial neural networks trained respectively to separate neutral and charged particles of b decays from fragmentation particles. In order to reconstruct the boost of the b-hadron, the three-momentum vector of the neutrino is estimated from the missing momentum in the lepton hemisphere and it is added to the momentum of the lepton and the momenta of the selected decay particles. A momentum and angular resolution of 4.5 GeV/c and 60 mrad respectively, are obtained. The discrimination between the $b \to X_u \ell\nu$ signal decays and the $b \to X_c \ell\nu$ background is based on the fact that the mass of the c quark is heavier than that of the u quark, leading to different kinematic properties for the two final states. Twenty variables, characterizing both the leptonic and the hadronic part, are combined in an artificial neural network NN_{bu} with a reduced sensitivity to the composition of the X_u system. The network outputs, as obtained from simulation and compared to data, are shown in figure 11 and 12.

The branching ratio is fitted from the NN_{bu} distribution of the data, with a binned likelihood fit, in the region $0.6 < \mathrm{NN}_{bu} < 1$, where 50% of the signal is expected to lay. In this region an excess of 303 ± 88 events is found. The result of

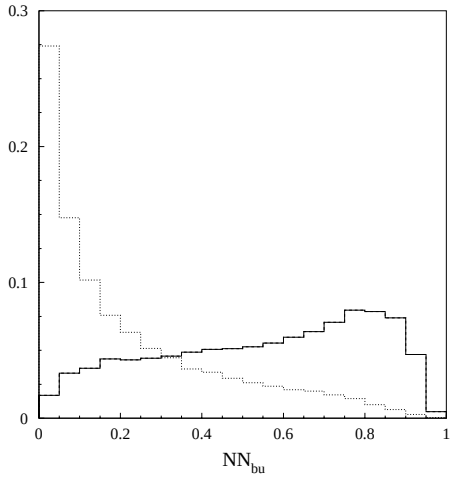

Figure 11: ALEPH analysis: output of the NN_{bu} for signal $b \to X_u \ell\nu$ transitions (solid line) and $b \to c$ background (dotted line). The two Monte Carlo distributions are normalized to the same area.

the fit is:

$$BR(b \to X_u \ell\nu) = (1.73 \pm 0.55(stat) \pm 0.51(syst\ b \to c) \pm 0.21(syst\ b \to u)) \times 10^{-3}$$

The systematic uncertainties have been separated in contributions due to the $b \to c$ transitions and those due to the modelling of $b \to u$ transitions and are described in table 3. The cut on NN_{bu} induces only small distortions on the lepton momentum distribution and on the hadronic mass spectrum. The residual model dependence has been studied varying all the parameters in the model used to simulate the signal. This is an hybrid model [26] where resonant states are considered at low hadronic energy, while for large energy non-resonant multipion final states are expected to dominate.

One candidate event $B^0 \to \rho^- e^+ \nu_e (\rho^- \to \pi^- \pi^0)$ is shown in figure 13.

The L3 measurement of $|V_{\mathrm{ub}}|$ is also an inclusive reconstruction of $b \to X_u \ell\nu$ events. The selection criteria to enhance the $b \to X_u \ell\nu$ signal over the background are based on cuts on eight discriminant variables constructed with the four-momenta of the lepton and of the two most energetic particles contained in the same hemisphere of the lepton. The combined system of the lepton and the most energetic particle is a better

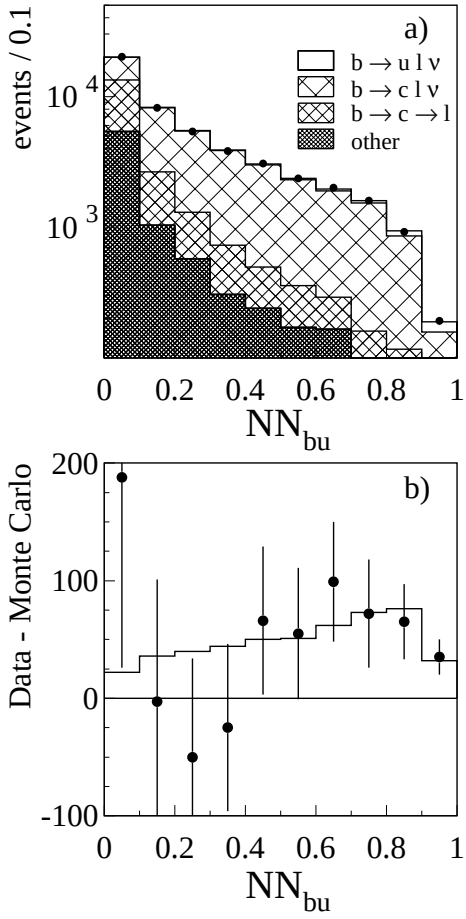

Figure 12: ALEPH analysis: neural network output NN_{bu} (a) comparison between data (points) and Monte Carlo (histogram), (b) difference between data and Monte Carlo with no $b \to u$ contribution (histogram)

approximation to the b-hadron in $b \to X_u \ell\nu$ than in $b \to X_c \ell\nu$ transitions, since less particles are missing in this approximation.

The efficiency for $b \to X_u \ell\nu$ is 1.5 % and an excess of 81 events is found after the application of all selection cuts. The measured branching ratio is:

$$BR(b \to X_u \ell\nu) = (3.3 \pm 1.0(stat) \pm 1.66(syst\ b \to c) \pm 0.55(syst\ b \to u)) \times 10^{-3}$$

A breakdown of the systematic uncertainties is presented in table 4.

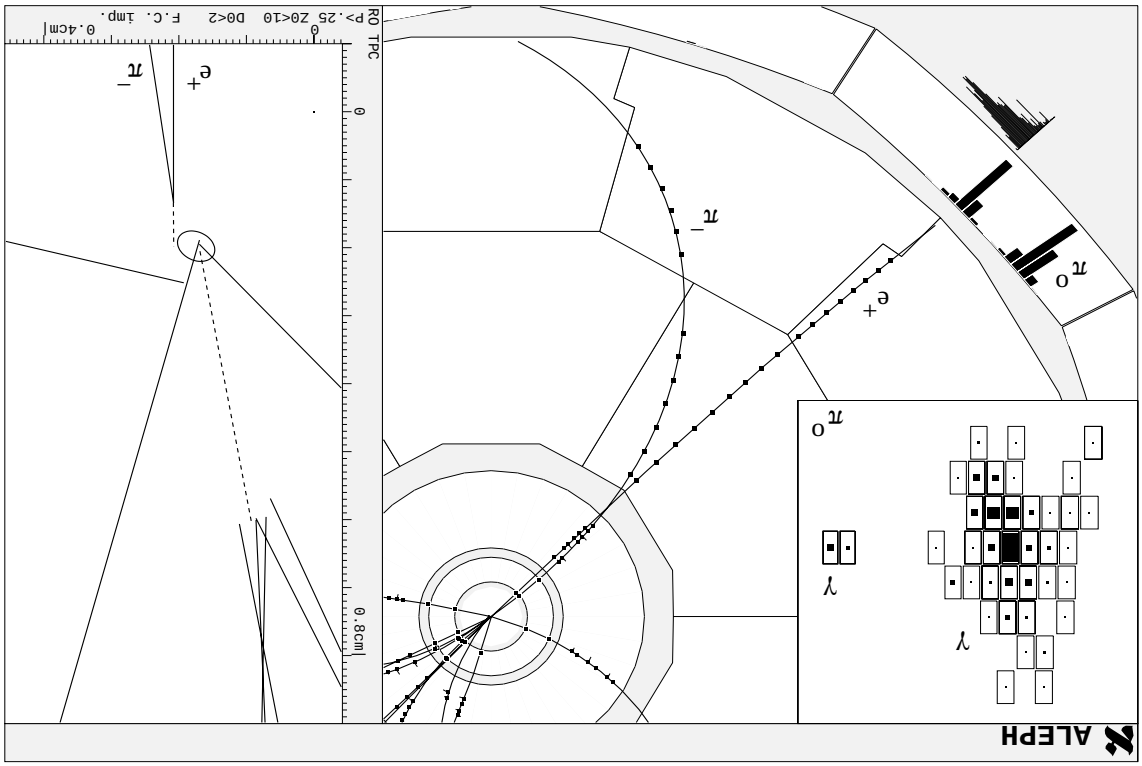

Figure 13: View of the scanned $B^0 \to \rho^- e^+ \nu_e$ event, with $\rho^- \to \pi^- \pi^0$ and $\pi^0 \to \gamma\gamma$. The right plot shows a close up $r\phi$ view of the interaction point and the upper left insert shows the energy deposited in the electromagnetic calorimeter by the photons coming from the π^0 decay.

Source	Δ BR($b \to X_u \ell \nu$)
b-hadron production	$\pm$ 0.16 10^{-3}
b-hadron decay	$\pm$ 0.31 10^{-3}
c-hadron decay	$\pm$ 0.37 10^{-3}
lepton identification	$\pm$ 0.08 10^{-3}
Total $b \to c$ uncertainty	$\pm$ 0.51 10^{-3}
Hybrid model cutoff	$\pm$ 0.08 10^{-3}
Exclusive model	$\pm$ 0.05 10^{-3}
Inclusive model	$\pm$ 0.18 10^{-3}
Λ_b modelling	$\pm$ 0.04 10^{-3}
Total $b \to u$ uncertainty	$\pm$ 0.21 10^{-3}

Table 3: Main estimated contributions to the systematic uncertainty on the ALEPH measurement of BR($b \to X_u \ell \nu$).

Source	Δ BR($b \to X_u \ell \nu$)
b-hadron production	$\pm$ 0.68 10^{-3}
b-hadron decay	$\pm$ 1.42 10^{-3}
Detector effects	$\pm$ 0.52 10^{-3}
Total $b \to c$ uncertainty	$\pm$ 1.66 10^{-3}
Monte Carlo statistics	$\pm$ 0.06 10^{-3}
Exclusive π rate	$\pm$ 0.19 10^{-3}
lepton spectrum	$\pm$ 0.04 10^{-3}
π spectrum	$\pm$ 0.27 10^{-3}
Λ_b rate	$\pm$ 0.43 10^{-3}
Total $b \to u$ uncertainty	$\pm$ 0.55 10^{-3}

Table 4: Main estimated contributions to the systematic uncertainty on the L3 measurement of BR($b \to X_u \ell \nu$).

Figure 14 shows the lepton momentum spectrum in the B rest frame for events passing the final selection in the $b \to X_u \ell \nu$ Monte Carlo sample, demonstrating that this analysis is sensitive to a large fraction of the spectrum.

As a cross check of the result, the eight discriminant variables have been combined in an artificial neural network, whose output is shown in figure 15, obtaining compatible results.

DELPHI has performed a determination of

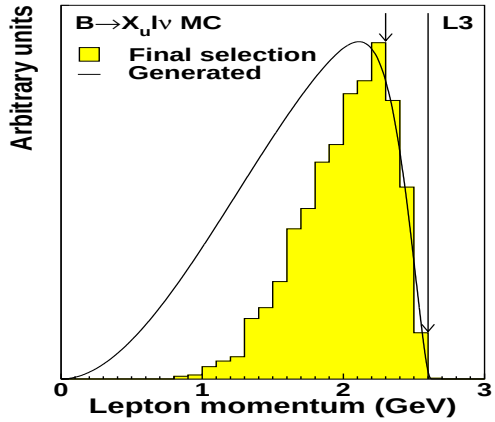

Figure 14: The Monte Carlo lepton momentum spectrum for the $b \to X_u \ell\nu$ transitions in the B rest frame. The curve shows the generated spectrum and the histogram the spectrum after the final selection. The arrows show the momentum range forbidden for $b \to X_c \ell\nu$ transitions.

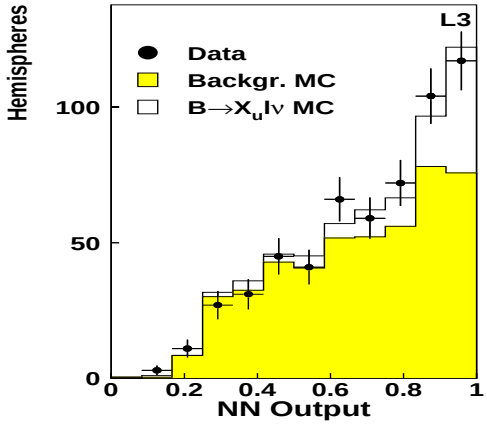

Figure 15: The neural network output distribution for the hemispheres selected by the final selection criteria for the data, the background and the signal Monte Carlo samples.

the ratio $|V_{\rm ub}/V_{\rm cb}|$[27] by a fit to the shape of the full spectrum of the lepton energy in the B rest frame, for b semileptonic decays with reconstructed hadronic invariant mass significantly smaller than the D mass. The reconstruction of the secondary hadronic system was performed with an inclusive method, using as a seed the identified lepton. Samples enriched and depleted in $b \to u$ transitions have been defined using two criteria. The first criterion considers the secondary vertex topology. The impact parameter w.r.t. the secondary vertex is computed for each lepton and a sign is attributed using the lifetime convention: it is signed negative if it appears to originate between the primary and the secondary vertex and positive if it originates in front of the secondary vertex. In $b \to X_c \ell\nu$ decays the secondary vertex corresponds to the D decay vertex, therefore leptons originating at the B decay vertex should appear with negatively signed impact parameters. On the contrary, in $b \to X_u \ell\nu$ transitions the secondary vertex coincides with both the B decay vertex and the lepton production point, therefore the impact parameter signing depends only on resolution effects. Decays with a significantly negative lepton impact parameter were assigned to a $b \to u$ depleted class. The second criterion considers that the presence of identified kaons in the same hemisphere as the lepton is an indication of a cascade decay $b \to c$ followed by a $c \to s$ decay, while in $b \to u$ transitions the presence of strange particles is suppressed. The invariant mass M_X of the reconstructed secondary hadronic system for enriched and depleted $b \to u$ events is shown in figure 16.

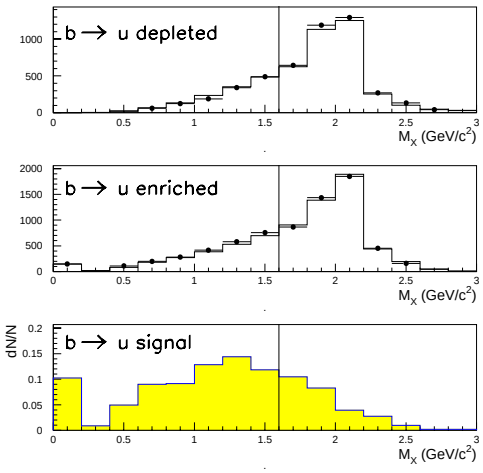

Figure 16: DELPHI analysis: invariant mass M_X of the reconstructed secondary hadronic system in selected decays for real data (points with error bars) and simulation (histogram). Upper plot: $b \to u$ depleted sample, medium plot: $b \to u$ enriched sample and lower plot: $b \to u$ signal.

The distribution of the lepton energy in the B rest frame, for events with small hadronic invariant mass is shown in figure 17 and 18.

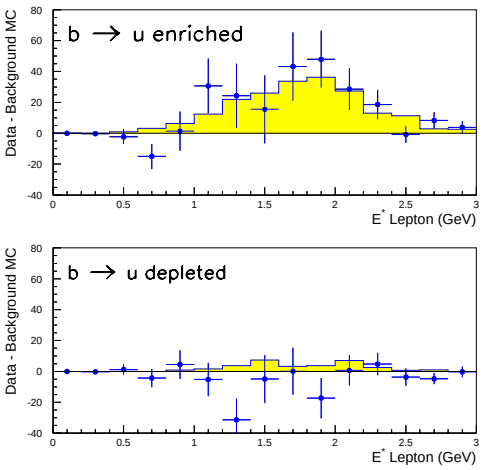

Figure 17: DELPHI analysis: background subtracted E^* distributions for events with an hadronic invariant mass $M_X < 1.6$ GeV/c^2. Upper plot: $b \to u$ enriched decays. Lower plot: $b \to u$ depleted decays. The shaded histograms show the expected E^*_ℓ distribution for signal decays normalized to the amount of signal corresponding to the fitted $|V_{\rm ub}/V_{\rm cb}|$ value.

The number of selected events and their E^* distribution have been used to extract the value of $|V_{\rm ub}/V_{\rm cb}|$ by a simultaneous binned maximum likelihood fit to the different samples of events, obtaining the following result:

$$|V_{\rm ub}/V_{\rm cb}| = 0.100 \pm 0.011(stat) \pm 0.018(syst) \pm 0.009(model)$$

A breakdown of the systematic uncertainties is presented in table 5.

Alternatively, the value of $|V_{\rm cb}|$ has been fixed to extract the $b \to X_u \ell\nu$ branching ratio:

$$BR(b \to X_u \ell\nu) = (1.56 \pm 0.38(stat) \pm 0.52(syst) \pm 0.23(model)) \times 10^{-3}$$

The average BR$(b \to X_u \ell\nu)$ at LEP has been calculated taking into account the correlation between experiments in the modelling of $b \to c$ and

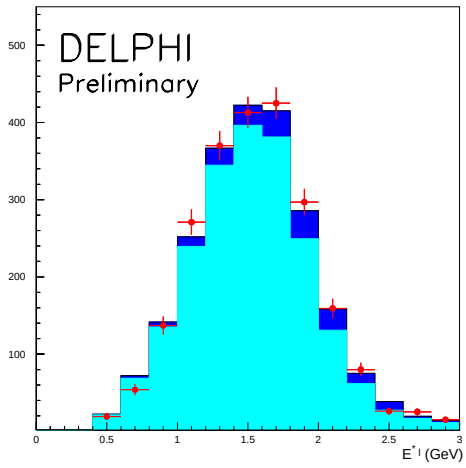

Figure 18: E^* distribution for the decays in the $b \to u$ enriched class with $M_X < 1.6$ GeV/c^2. Points with errors bars: data, light shaded histogram: backgrounds, dark shaded histogram: signal normalized to the fitted fraction of events.

Error source	Δ ($\lvert V_{\rm ub}/V_{\rm cb}\rvert$)
charm decay	$\pm$ 0.009
b-hadron production and decay	$\pm$ 0.011
Detector effects	$\pm$ 0.010
$b \to u$ modelling	$\pm$ 0.009

Table 5: Main estimated contributions to the systematic uncertainty on the DELPHI measurement of $|V_{\rm ub}/V_{\rm cb}|$

$b \to u$ transitions. The result, as shown in figure 19, is:

$$BR(b \to X_u \ell\nu) = (1.67 \pm 0.35(stat) \pm 0.38(syst\ b \to c) \pm 0.20(syst\ b \to u)) \times 10^{-3}$$

In order to extract the value of the $|V_{\rm ub}|$ matrix element, the following expression is used [24, 1]:

$$|{\rm V_{ub}}| = 0.00445 \sqrt{\frac{BR(b \to X_u \ell\nu)}{0.002} \frac{1.55}{\tau_b}} \times (1 \pm 0.010(pert) \pm 0.035(m_b) \pm 0.030(\frac{1}{m_b^3}))$$

where τ_b is the world average value of the b-hadron lifetime: $\tau_b = 1.564 \pm 0.014$ ps. The

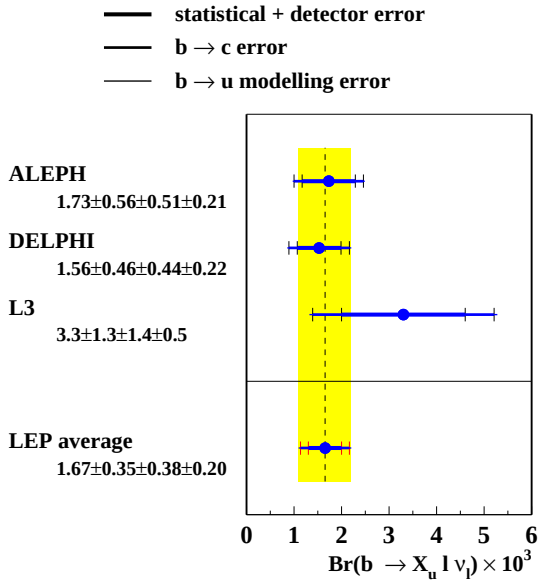

Figure 19: Average of BR($b \to X_u \ell\nu$) values measured at LEP.

result is:

$$|\mathrm{V_{ub}}| = (4.05^{+0.62}_{-0.74}) \times 10^{-3}$$

4. Constraints on Unitarity Triangle

As an example of the power of the presented measurements to constrain the parameters of the Unitarity Triangle, the results obtained in reference [29] are reported here. The method used consists of determining the $\bar{\rho}$ and $\bar{\eta}$ values by building up their two dimensional probability distributions. The errors on the measurements are taken as having either Gaussian or uniform distributions, depending on the source of the error. The complete table of input quantities can be found in [29]. Figure 20 shows the allowed regions in the ($\bar{\eta}$, $\bar{\rho}$) plane with and without including the constraint coming from K^0 measurements. The fitted values, including the constraint coming from K^0 measurements, are:

$$\bar{\rho} = 0.214^{+0.055}_{-0.062} \qquad \bar{\eta} = 0.340 \pm 0.040$$

It is remarkable that the probability for $\bar{\rho}$ to lie in the negative plane region is smaller than 1%.

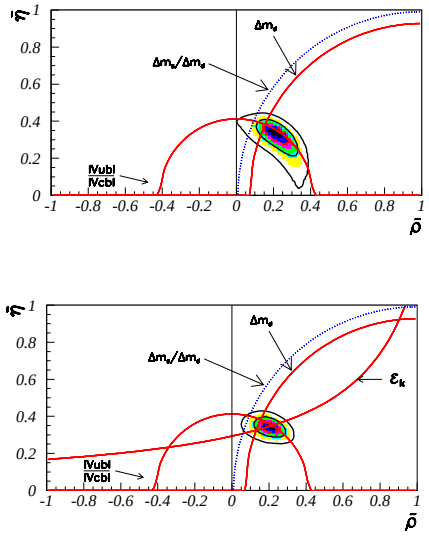

Figure 20: Constraints in the $\bar{\eta}$,$\bar{\rho}$ plane. In the upper plot the constraint coming from K^0 measurements is not included. The 68% and 95% CL contours are shown.

5. Conclusions

New measurements have been performed by the four LEP Collaborations with data collected at LEP at the Z^0. The average result obtained for the $|V_{\mathrm{cb}}|$ element from inclusive and exclusive measurements is:

$$|\mathrm{V_{cb}}| = (40.2 \pm 1.9) \times 10^{-3} \qquad (5.1)$$

From inclusive charmless semileptonic b-hadron decays the average value of $|\mathrm{V_{ub}}|$ is:

$$|\mathrm{V_{ub}}| = (4.05^{+0.62}_{-0.74}) \times 10^{-3}$$

Acknowledgments

I would like to thank all the members of the LEP $|V_{\mathrm{cb}}|$ and $|V_{\mathrm{ub}}|$ working groups for their excellent work and the help they gave me in preparing this talk. I am also indebted to A. Stocchi for providing me with the results on the $\bar{\eta}$, $\bar{\rho}$ parameters.

References

[1] *Combined results on b-hadron production rates, lifetime, oscillations and semileptonic decays*, LEPHF note 99-02, document in preparation. See also `http://www.cern.ch/LEPHFS/`.

[2] LEP/SLD Electroweak Working Group, Electoweak Results Presented at the 1999 Summer Conferences, document in preparation.

[3] *Measurement of the semileptonic b branching ratios in Z decays*, DELPHI Collaboration, DELPHI 99-111 CONF 298, contributed paper # 5-522 to the *HEP'99* Conference, Tampere (Finland), July 15-21 1999.

[4] *Measurement of inclusive semileptonic branching fractions of b hadrons in Z0 decays*, OPAL Collaboration, CERN-EP/99-078 and Contributed paper # 5-11 to the *HEP'99* Conference, Tampere (Finland), July 15-21 1999.

[5] *Measurement of Rb and BR($b \to \ell\nu X$) at LEP Using Double-Tag Methods*, L3 Collaboration, L3 note 2420, contributed paper # 5-282 to the *HEP'99* Conference, Tampere (Finland), July 15-21 1999.

[6] *Measurement of the semileptonic b branching ratios from inclusive leptons in Z decays*, ALEPH Collaboration, contributed paper # 404 to the *HEP'95* Conference, Brussels (Belgium), July 1995.

[7] L3 Collaboration, M. Acciarri *et al.*, *Z. Physik* **C 71** (96) 379.

[8] I. I. Bigi, M. Shifman and N. Uraltsev, *Ann. Rev. Nucl. Part. Sci.* **47** (97) 591.

[9] N. Isgur and M. Wise, *Phys. Lett.* **B 232** (89) 113. N. Isgur and M. Wise, *Phys. Lett.* **B 237** (90) 527.

[10] A. F. Falk, H. Georgi, B. Grinstein and M. B. Wise, *Nucl. Phys.* **B 343** (90) 1.

[11] M. Luke, *Phys. Lett.* **B 252** (90) 447.

[12] I. Caprini and M. Neubert, *Phys. Lett.* **B 380** (96) 376.

[13] I. Caprini, L. Lellouch and M. Neubert, *Nucl. Phys.* **B 530** (98) 153.

[14] A. K. Leiboich, Z. Ligeti, I. W. Stewart and M. B. Wise, *Phys. Rev.* **D 57** (98) 308, [hep-ph/970567].

[15] BABAR Physics Book.

[16] A. Anasassov *et al.*, CLEO Collaboration, *Phys. Rev. Lett.* **80** (98) 4127

[17] D. Buskulic *et al.*, ALEPH Collaboration, *Z. Physik* **C 73** (97) 601

[18] A. Albrecht *et al.*, ARGUS Collaboration, *Z. Physik* **C 57** (93) 533

[19] *Measurement of the B Semileptonic Branching Fraction into Excited Charm Mesons*, DELPHI Collaboration, DELPHI 99-103 CONF 290, contributed # 5-514 to the *HEP'99* Conference, Tampere (Finland), July 15-21 1999.

[20] *New precise measurement of* $|V_{cb}|$, DELPHI Collaboration, DELPHI 99-107 CONF 294, contributed # 4-518 to the *HEP'99* Conference, Tampere (Finland), July 15-21 1999.

[21] D.Buskulic *et al.*, ALEPH Collaboration, *Phys. Lett.* **B 395** (1997) 373.

[22] K. Ackerstaff *et al.*, OPAL Collaboration, *Phys. Lett.* **B 395** (1997) 128.

[23] C. Caso *et al.*, Particle Data Group, *Eur. Phys. J.* **C3** (1998) 1.

[24] N. Uraltsev *et al.*, *Eur. Phys. J.* **C4** (1998) 453 and update in N. Uralsev, [hep-ph/9905520]
A. H. Hoang, Z. Ligeti and A. V. Manohar, *Phys. Rev. Lett.* **82** (99) 277 and
A. H. Hoang, Z. Ligeti and A. V. Manohar, *Phys. Rev.* **D 59** (99) 074017.

[25] R. Barate *et al.*, ALEPH Collaboration, *Eur. Phys. J.* **C6** (1999) 555.

[26] C. Ramirez, J. F. Donoghue and G. Burdman, *Phys. Rev.* **D 41** (90) 1496.

[27] *Measurement of BR($b \to X_u \ell\nu$) and determination of* $|V_{ub}/V_{cb}|$ *with DELPHI at LEP*, DELPHI Collaboration, DELPHI 99-119 CONF 297, contributed paper # 4-521 to the *HEP'99* Conference, Tampere (Finland), July 15-21 1999.

[28] M. Acciarri *et al.*, L3 Collaboration, *Phys. Lett.* **B 436** (98) 174.

[29] F. Parodi, P. Roudeau, and A. Stocchi, LAL99-03 [hep-ex/9903063].